Gold Nanostar–polymer Hybrids for siRNA Delivery: Polymer Design Towards Colloidal Stability and in vitro Studies on Breast Cancer Cells

Carla Sardo[a], Barbara Bassi[b], Emanuela F. Craparo[a], Cinzia Scialabba[a], Elisa Cabrini[b], Giacomo Dacarro[b], Agnese D'Agostino[b], Angelo Taglietti[b], Gaetano Giammona[a], Piersandro Pallavicini[b§]*, Gennara Cavallaro[a§]*.

[a]Laboratorio di Polimeri Biocompatibili, Dipartimento di Scienze e Tecnologie Biologiche, Chimiche e Farmaceutiche (STEBICEF), Sezione di Chimica e Tecnologie Farmaceutiche, Università degli Studi di Palermo, Via Archirafi 32, 90123 Palermo, Italy

[b]Dipartimento di Chimica, Università di Pavia, viale Taramelli, 12 - 27100 Pavia, Italy

*Corresponding Authors:

Gennara Cavallaro
E-mail: gennara.cavallaro@unipa.it
Dipartimento di Scienze e Tecnologie Biologiche , Chimiche e Farmaceutiche (STEBICEF)
Università degli Studi di Palermo
Via Archirafi 32, 90123, Italia

Piersandro Pallavicini
E-mail: piersandro.pallavicini@unipv.it
Dipartimento di Chimica,
Università di Pavia,
viale Taramelli, 12 – 27100 Pavia, Italy
§ Contributed equally to the work

Abstract

To overcome the low bioavailability of siRNA and to improve their transfection efficiency, the use of non-viral delivery carriers is today a feasible approach to transform the discovery of these incredibly potent and versatile drugs into clinical practice. Polymer-modified gold nanoconstructs (AuNCs) are currently viewed as efficient and safe intracellular delivery carriers for siRNA, given the possibility to conjugate the ability to stably entrap and deliver siRNAs inside cells and the advantages of gold nanoparticles as theranostic agents and radiotherapy enhancers trough laser-induced hyperthermia.

In this study, AuNCs were prepared by coating Gold Nano Stars (GNS) with suitable functionalised polymers to give new insight on the choice of the coating in order to obtain colloidal stability, satisfying in vitro transfection behaviour and reliability in terms of homogeneous results upon GNS type changing. For this goal, two different polymers were used to coat GNS of three different size and shape: i) α-mercapto-ω-amino polyethylene glycol 3000Da (SH-PEG_{3000}-NH_2), a hydrophilic linear polymer; or ii) PHEA-PEG_{2000}-EDA-LA (PPE-LA), an amphiphilic hydroxyethylaspartamide copolymer containing PEG. Both polymers contain -SH or –SS- groups for anchoring on gold surface and NH_2 protonable groups to obtain a positive surface for siRNA layering. The coating polymers features on siRNA layering and the extent of intracellular uptake and luciferase gene silencing effect were evaluated for each of the obtained coated GNS. Obtained results highlight that amphiphilic biocompatible polymers with multi-grafting function are more suitable for assuring the colloidal stability and effectiveness of these colloidal systems with respect to a linear PEG coating.

Keywords: PHEA, PEG, lipoic acid, Gold Nanostars, siRNA delivery, MCF-7

1. Introduction

The growing families of gold nanoparticles (AuNPs), that comprise gold nanostars, nanorods, nano-pyramids, nanocages, nanospheres and other shapes, possess interesting features. These are due to favourable properties such as a bio-inert surface, easily modifiable surface chemistry, a high degree of control on size and shape during synthesis and remarkable features such as light scattering, intense absorptions bands due to localized surface plasmon resonance (LSPR) and photothermal effects due to irradiation on their LSPR bands, either in the visible or in the bio transparent Near IR (NIR) (Huang et al., 2008). Other well-known features of AuNPs include chemical inertness, neglibile toxicity, and high conjugation efficiency of various biomolecules and biocompatible polymers with the formation of AuNanoconstructs (AuNC), a promising platform for various biomedical applications and in particular for cancer treatment (Lee et al., 2014; Muddineti et al., 2015). AuNC can accumulate in tumour tissue either passively or actively. Passive accumulation takes place via the Enhanced Permeability and Retention (EPR) effect (Greish, 2010), a selective high local concentration of nano-sized anticancer drugs in tumour tissues due to abnormalities of tumour vasculature (namely hyper vascularization, aberrant vascular architecture, extensive production of vascular permeability factors stimulating extravasation within tumour tissues, and lack of lymphatic drainage). Active accumulation takes place via AuNC conjugation with a targeted molecule, specifically recognised by an hyper expressed receptor.

Through LSPR, AuNC based on non-spherical AuNP can induce through-tissues hyperthermia with NIR laser (Huang et al., 2008). Gold's high atomic number enables it to enhance the effect of radiotherapy, which in turn can be amplified by mild, laser-induced hyperthermia. Conjugated with drugs, AuNC can also be drug carriers able to enhance the uptake of the drug in the tumour tissue and controlled release of the drug may be switched or enhanced by hyperthermal stimulation. An additional attractive feature of AuNPs is their affinity for thiols, due to the high stability of the Au-thiolate bond, providing an effective and

selective means of controlled glutathione-mediated payload release via place-exchange reaction inside cells (Ghosh et al., 2008).

Gold nanostars (GNS) are branched gold nanoparticles with LSPR absorptions tunable in the NIR range, including in the bio-transparent window (750-1100 nm). Interest in GNS has increased because of the ease of synthesis for large scale production, high surface-to-volume ratio useful for improving drug loading efficiency, huge SERS effects due to the sharp branch edges, (Guerrero-Martínez et al., 2011) and use of their TPL (two-photon luminescence) when irradiated in the NIR for deep tissue imaging (Liu et al., 2015). Their photothermal response on NIR irradiation is particularly efficient, (Freddi et al., 2013). It was also reported that gold nanostars functionalized with TAT-peptides efficiently internalize in cells and it was demonstrated that these particles are promising agents for cancer therapy via photothermolysis (Yuan et al., 2012).

The potential of RNA interference (RNAi)-based therapeutics for cancer has received much attention. However, delivery of RNAi effectors, such as small interfering RNA (siRNA), remains an obstacle to clinical translation. Among non-viral delivery vectors that have been investigated, AuNC with different size, shape, structure, chemistry and synthetic strategies have shown potential to enhance siRNA delivery in vitro and in vivo (Lee et al., 2008; Perche et al., 2016; Rahme et al., 2015; Wang et al., 2016; Zhao et al., 2015). It was also recently found that interferon-β levels in macrophage cells after treatment with densely functionalized oligonucleotide-modified gold nanoparticles was up to 25-fold less when compared to treatment with a lipoplex carrying the same oligonucleotide sequence, stating their significant lower innate immune response than those produced by some conventional DNA transfection materials (Massich et al., 2009). In this study, three GNS types belonging to three dimensional ranges (GNS TRITON: 80-90 nm; GNS LSB: 50-70 nm; shrunk GNS LSB: 20-30 nm, see **Figure 1**) were synthesised, characterized and coated with two different polymers for intracellular siRNA delivery. Such nanoparticles belong to the GNS typology widely used

by our groups, i.e. prepared with seed-growth syntheses in water using weakly interacting surfactants (lauryl sulfobetaine for GNS LSB, (Casu et al., 2012) and TritonX-100 for GNS TRITON (Pallavicini et al., 2013) as the protecting and directing agents. The weak surfactant-Au interaction allows their facile complete elimination after GNS growth, by coating GNS surfaces with functional thiols. In particular, we used SH-PEG_{3000}-NH_2 (Mw = 3000 Da) and PHEA-PEG_{2000}-EDA-LA (PPE-LA). The latter is an amphiphilic hydroxyethylaspartamide-based copolymer prepared by our groups (Cavallaro et al., 2013), with interesting features such as biocompatibility and functionalization with 1,2-dithiolane rings, PEG chains and amino groups as backbone pendent moieties. These features enable PPE-LA to coat GNS, to complex siRNAs and to ensure an hydrophilic PEG shielding for stealth properties and stability. Together with these interesting features and differently from SH-PEG_{3000}-NH_2, PPE-LA is not a telechelic polymer, but is a branched multifunctional copolymer thus having an higher density of protonable amines and many functionalizable groups (dithiolane rings, primary amines and hydroxyls) on the structure, enabling the linkage of further specific ligands. These may include active targeting agents to increase the siRNA uptake in a target cell population and to decrease the uptake in off-target cells and organs, endosomal escape agents to increase and fasten the siRNA release in the cell cytoplasm, and stimuli-responsive moieties to control drug biodistribution in response to endogenous variations (changes in pH, enzyme concentration, redox gradients etc.).

The features of polymer-coated GNS upon siRNA layering, in terms of size and surface charge, colloidal stability and extent of intracellular uptake and luciferase gene silencing effect, were evaluated on MCF-7/Luc cells for each of the coated GNS obtained to explore and compare their potential as intracellular siRNA carriers. Moreover cytocompatibility studies were carried out on the same model cell line.

2. Material and methods

2.1. Chemicals and Instrumentation

Lauryl sulfobetaine (LSB), Triton X-100, tetrachloroauric acid 30% wt. in HCl, sodium borohydride ≥98%, ascorbic acid ≥99%, silver nitrate ≥99%, D,L-Aspartic acid, ethanolamine, ethylenediamine, O-(2-Aminoethyl)-O′-methylpolyethylene glycol (2000 Da), diethyl ether, acetone, 1-butanol, anhydrous N,N-Dimethylformamide, Bis(4-nitrophenyl)carbonate, α-lipoic acid, N-(3-Dimethylaminopropyl)-N′-ethylcarbodiimide hydrochloride, N-Hydroxysuccinimide, were all purchased from Sigma-Aldrich and used without further purification. SH-PEG_{3000}-NH_2 (α-mercapto-ω-amino polyethylene glycol) was purchased from RAPP Polymere. Bidistilled water was used in all preparations not containing siRNA. siRNA dilutions were made by employing RNase-free molecular biology grade water.

UV-Vis spectra were taken on Cary 60 Varian, using poly(methyl methacrylate) cuvettes (optical path 1 cm). Ultracentrifugation was carried out using a HermleZ366 ultracentrifuge with polypropylene 10 mL tubes at 13000 rpm (15870 g). Zeta potential was measured with a Zetasizer Nano ZS90 Malvern instrument, equipped with a dedicated cuvette. TEM images were taken with Jeol JEM-1200 EX II instrument on 10 μL colloidal solution drops, deposited on copper grids (300 mesh) covered with a Parlodion membrane.

Duplexed siRNA, siGL3 (MW 13300), were purchased from eurofins MWG operon (Ebersberg). The sequence of the sense strand (5'→3') is reported herewith below: Luciferase GL3 CUUACGCUGAGUACUUCGA(dTdT), with and without Cy5 linked to the 5'-end. Cy5 is Cyanine5, a chromophore and fluorophore (see **Figure S4** of Supplementary material for structure) with absorption maximum at λ 550 nm and emission maximum at λ 570 nm.

2.2. Synthesis of GNS LSB

The synthesis of GNS was carried out with an already described seed-growth approach using the Lauryl Sulphobetaine (LSB) zwitterionic surfactant (Casu et al., 2012). In brief, the seed

solution was prepared in a vial: 5 mL of $HAuCl_4$ $5 \cdot 10^{-4}$ M in water were added to 5 mL of an aqueous solution of LSB 0.2 M; thereafter the solution was gently hand-shaken and a pale yellow colour appeared. Then 600 μL of an ice-cooled solution of $NaBH_4$ 10^{-2} M in water were added and the solution was gently hand-shaken. Immediately an orange-brown colour appeared. The seed solution was kept in ice and used within 4 hours. The growth solution was prepared in a flask. To 50.0 mL of 0.2M LSB aqueous solution, 1.800 mL of $AgNO_3$ $4 \cdot 10^{-3}$ M in water, 50.0 mL of $HAuCl_4$ $5 \cdot 10^{-4}$ M in water, 0.800 mL of ascorbic acid 0.0788 M in water and 0.120 mL of the seed solution were added in this order. After gentle mixing, a pink colour appeared and quickly changed to blue and became more intense. The sample was allowed to equilibrate for 1 h at room temperature. After this time the solution was ultracentrifugated (13000 rpm, 15870 g, 25'), the supernatant discarded and the precipitate resuspended in 100 mL of water. The UV-Vis extinction spectrum of such product was recorded using a 1 cm cuvette.

2.3. Synthesis of shrunk GNS LSB

The synthesis was carried out as described for GNS LSB, except for an increased quantity of added seed solution i.e. 0.250 mL (instead of 0.120 mL). After such an addition and gentle mixing, a pink colour appeared that quickly changed to blue. The sample was allowed to equilibrate for 1 h at room temperature. After this time the solution was ultracentrifugated (13000 rpm, 15870 g, 25'), the supernatant discarded and the precipitate resuspended in 10 mL of water. The UV-Vis extinction spectrum of such product was recorded using a 1 mm cuvette.

2.4. Synthesis of GNS TRITON

The synthesis of GNS TRITON was carried out with a seed-growth approach using a synthesis already described by some of use employing the nonionic TritonX-100 surfactant

(Pallavicini et al., 2013). Briefly, first a seed solution was prepared in a vial with 5.00 mL of $HAuCl_4$ $5 \cdot 10^{-4}$ M in water that were added to 5.00 mL of an aqueous solution of Triton X-100 0.2 M. Thereafter the solution was gently hand-shaken and a pale yellow colour appeared. Then 600 μL of an ice-cooled solution of $NaBH_4$ 10^{-2} M in water were added, the solution was gently hand-shaken and an orange-brown colour soon appeared. The seed solution was kept in ice and used within 3 hours. The growth solution was prepared in a flask. To 50.0 mL of a 0.2M aqueous solution of TritonX-100, 2.500 mL of $AgNO_3$ $4 \cdot 10^{-3}$ M in water, 50.0 mL of $HAuCl_4$ $5 \cdot 10^{-4}$ M in water, 1.600 mL of ascorbic acid 0.0788 M in water and 0.120 mL of the seed solution were added in this order. After gentle mixing a pink colour appeared and quickly changed to blue-green and became more intense. The sample was allowed to equilibrate for 1 h at room temperature. Due to the particularly weak GNS-TritonX-100 interactions, no ultracentrifugation is allowed at this stage of the synthesis, as it would lead to aggregation (repeated ultracentrifugation was carried out on the coated GNS for purification). A UV-Vis extinction spectrum of such product was recorded using a 1 cm cuvette.

2.5. Synthesis of PHEA-PEG$_{2000}$-EDA-LA

PHEA-PEG$_{2000}$-EDA-LA (PPE-LA) was synthesized according to the previously described procedure (Cavallaro et al., 2013).

2.6. Coating with SH-PEG$_{3000}$-NH$_2$ or PPE-LA

To 100 mL of GNS suspension (GNS LSB; shrunk GNS LSB; GNS TRITON), 2.5 mL of a 10^{-3} M stock solution in water of the chosen polymer was added. The polymer final concentration was thus $2.5 \cdot 10^{-5}$ M. After addition of the chosen polymer, the solutions were stirred for 1h at room temperature, then ultracentrifugated (13000 rpm, 15870 g, 25'). The supernatant was discarded and the precipitate redissolved in the same starting volume with bidistilled water. Ultracentrifugation and redissolution cycles were repeated 2 more times, to

guarantee the elimination of the surfactant and of the polymers not grafted on the GNS surface. After the last ultracentrifugation, the GNS pellets were redissolved in 10 mL of water instead of 100, in order to obtain a 10X increased concentration. UV-Vis absorption spectra were recorded on these solutions, using 1 mm quartz cuvettes.

2.7. ICP-OES (inductively coupled plasma optical emission spectroscopy) analysis

GNS LSB and GNS TRITON, coated with different polymers, were prepared according to the already described procedure. After the last ultracentrifugation cycle, the pellet was treated with 1 mL *aqua regia* and after complete reaction (1 hour, solid dissolution and colour disappearance) the obtained solution was diluted with 2 mL bidistilled water. The Au concentration was then determined by ICP-OES on an ICP-OES OPTIMA 3000 Perkin Elmer instrument.

2.8. Preparation of coated-GNS/siRNA complexes

In order to obtain coated-GNS/siRNA complexes 100 µL of coated-GNS aqueous stock dispersion were mixed with 100 µL of siRNA aqueous solutions at various concentrations in order to obtain different siRNA/gold weight ratios. The mixtures were incubated at room temperature for at least 2h to allow complex formation. Au concentrations of the various coated-GNS types are listed in SI3 and range from 0.17 to 0.33 mg/mL.

2.9. Size and ζ potential measurements

Dynamic light scattering studies (DLS) were performed at 25 °C with a Malvern Zetasizer Nano ZSP instrument fitted with a 532 nm laser at a fixed scattering angle of 173°, using the Dispersion Technology Software 7.02. The intensity-average hydrodynamic diameter (nm), and polydispersity index (PDI) were obtained by cumulative analysis of the correlation function. Samples were then diluted with 400 µL of nuclease free bidistilled water and used to

determine the Zeta potential. Zeta potential measurements were performed by aqueous electrophoresis measurements, recorded at 25 °C using the same apparatus. The zeta potential values (mV) were calculated from the electrophoretic mobility using the Smoluchowsky relationship.

2.10. Cell culture and reagents

Biological evaluations were conducted on human breast carcinoma cell line stably transfected to express firefly luciferase gene (MCF-7/Luc, Cell Biolabs Inc. San Diego). MCF-7/Luc cells were grown in Dulbecco's modified Eagle's medium (DMEM) with 10% foetal bovine serum (FBS), 1% of glutamine and 1% of penicillin/streptomycin (100 U/mL penicillin and 100 mg/mL streptomycin), at 37°C in 5% CO_2 humidified atmosphere. DMEM and the other cell culture constituents were purchased from Euroclone. CellTiter 96® AQueous One Solution Cell Proliferation Assay (MTS) was from Promega. Opti-MEM® I Reduced-Serum Medium was purchased from Life Technologies. Bicinchoninic Acid Kit for Protein Determination (BCA), Sodium dodecyl sulphate (SDS) and Triton X-100 were from Sigma Aldrich.

2.11. Cytocompatibility assay

MCF-7/Luc cells, were seeded in a 96 well plate at a density of $2 \cdot 10^4$ cells/well. After 24 hrs, 200 µL of fresh OPTI-MEM medium containing coated GNS/siRNA complexes at different siRNA to gold weight ratios, to reach a final siRNA concentration of 200 nM, were added to cells. Untreated cells were used as control with 100% viability. After 24 h of incubation, cells were washed with 100 µL of sterile DPBS and incubated with fresh DMEM containing 20 v% of MTS reagent. Plates were incubated at 37 °C for 2 h and after this time the absorbance of formazane was measured by a UV plate reader (AF2200, Eppendorf), at 492 nm. Wells filled with MTS reagents at the same concentration in DMEM were used as blank to calibrate the spectrophotometer to zero absorbance. The cell viability (%) compared to untreated control

cells were calculated by (*Abs* sample / *Abs* control) ×100 and represent mean ± standard deviation for triplicated samples.

2.12. Uptake studies

To determine quantitatively the cellular uptake of GNS/siRNA-Cy5 complexes, MCF-7/Luc cells were seeded in a 24 well plate at a density of $1.2 \cdot 10^5$ cells/well. After 24h, the culture medium was replaced by 600 µL of OPTI-MEM I medium containing coated GNS/siRNA-Cy5 complexes at different siRNA to gold weight ratios, to reach a final siRNA concentration of 200 nM. After 4h and 24h incubation, cells were extensively washed with sterile DPBS and lysed in 100 µL lysis buffer (2% SDS, 1% Triton X-100, in sterile DPBS). The lysates were divided in two parts: the first one (75 µL) was used to measure the fluorescence intensity of the Cy5 function by a Shimadzu RF-5301 PC spectrofluorophotometer (λ_{ex}: 647 nm; λ_{em}: 673 nm) calibrated with standard solutions of siGL3-Cy5 at various concentration ranging from 10 to 1000 nM; the second one (25 µL) was used to evaluate the total cellular protein amount by BCA protein assay. The results were expressed as the ratio nanograms siGL3 per milligram of protein.

2.13. In vitro gene silencing

Twenty four hours before experiment MCF-7/Luc cells were seeded in a 96 well plate at a density of $2 \cdot 10^4$ cells/well. The culture medium was then removed and replaced with 200 µL of OPTI MEM medium containing GNS/siRNA complexes prepared at various siGL3/gold weight ratios, ranging from 0.025 to 1, and obtaining a final siRNA concentration per well of 200 nM. After 24h of incubation cells were washed with sterile DPBS and incubated with fresh medium and lysed after further 24 h with 50 µL of Lysis Buffer 1X. Luciferase gene expression was analysed on 20 µL of lysates with the Luciferase Assay System (Promega), according to the product manual, using a GloMax 20/20 Luminometer (Promega). 25 µL of

cell lysates were used to determine the total cellular protein content by BCA protein determination assay. Transfection efficiencies of GNS/siRNA complexes with various weight ratios, expressed as % of cells with full luciferase expression normalized by protein content (RLU/mg protein %), were compared to each other and results are shown as relative mean values of replicate of 3 ± standard deviation.

2.14. Statistical analysis

A T Test was applied to compare different groups. Data were considered statistically significant with a value of $p < 0.05$. All values are the average of three experiments ± standard deviation.

3. Results

3.1. GNS synthesis and properties

Uncoated GNS were prepared according to well established procedures as already described by us (Casu et al., 2012; Pallavicini et al., 2013). In particular, we used seed-growth syntheses with highly concentrated, weakly interacting surfactants acting as protecting agent and directing agent. Such surfactants induce the non-spherical growth of gold nanoparticles by selectively adhering to given Au crystal faces of the forming nanoparticles, allowing Au(0) deposition on the free crystal faces and preventing aggregation. GNS are obtained instead of gold nanorods by using LSB and TritonX-100 instead of the strongly interacting Cetyl Trimethyl Ammonium Bromide, while maintaining all the other synthetic conditions unchanged (Nikoobakht and El-Sayed, 2003). At the end of the GNS growth process the weakly interacting surfactants can be easily and completely displaced from the Au surface by the addition of molecular coatings featuring thiol groups. These form stable Au-S coordinative bond with GNS (Borzenkov et al., 2015). If the grafted thiol belongs to a PEG polymer or a PEG-containing copolymer, a remarkable stabilization is obtained, allowing to

suspend the coated GNS in a range of solvents (water or non-aqueous) and in cell-growth medium (Casu et al., 2012; Pallavicini et al., 2015, 2013). The shape and the dimensions of the two GNS types are to be briefly illustrated. Under the used synthetic conditions GNS LSB are obtained as a mixture of pentatwinned branched nanoparticles (with 2-5 branches), that are the main component (~60-70%), and of four-branched monocrystalline nanoparticles (20%), with some additional spherical undeveloped objects (Casu et al., 2012; Pallavicini et al., 2011). The TEM image in **Figure 1A** visualizes the morphology of such two species, from a sample prepared for this work. The tip to tip distance is ~ 50 nm for the four-branched GNS and in the 60-70 nm range for the pentatwinned ones. Their extinction spectrum is dominated by the LSPR band of the pentatwinned species, whose position is regulated by synthetic conditions (regulating in turn the branches length to base ratio) and falling at ~ 800 nm in the conditions chosen for this work. The weaker LSPR of the monocrystalline species is the shoulder at 600-650 nm in **Figure 1D**, red spectrum.

GNS Triton under the chosen conditions are pentatwinned nanoparticles with five usually identical branches protruding from the core (Pallavicini et al., 2013), as illustrated by TEM, **Figure 1B**, on a sample used for this work. GNS TRITON have two Near IR LSPR absorptions whose position is regulated by synthetic conditions (regulating in turn the branches aspect ratio). Under the synthetic conditions chosen for this paper, one LSPR is at ~ 820 nm (see **Figure 1D**, blue spectrum) and the second is at ~ 1500 nm (not shown in **Figure 1D**). The tip to tip distance is 80-90 nm.

GNS LSB and GNS TRITON have different shapes, but in all cases their overall dimensions exceed those considered optimal for cell internalization, i.e. < 50 nm (Jiang et al., 2008). To obtain smaller GNS we modified the GNS LSB synthesis, increasing the seeds-to-Au ratio in the growing process by a 2.1 factor (see Experimental Section). Increasing the number of crystallization centres with the same quantity of starting Au(III) is expected to yield to a

larger number of GNS with less developed branches. Consistently, we obtained shrunk GNS LSB, i.e. with considerably lower overall (tip to tip) dimensions. The products are mixtures containing ~ 39% 4-branched monocrystalline GNS (tip-to-tip = 23 nm), ~ 20% 3-branched pentatwinned GNS (tip-to-tip 28 nm), ~ 38% apparently spherical nanoparticles (undeveloped pentatwinned crystals, d = 10 nm) plus an almost negligible quantity (<5%) of 2-branched pentatwinned GNS (tip to tip 56 nm), see **Figure S1(A-D)** and **Table S1** in Supplementary material for a complete set of TEM images and counting. A TEM image of the shrunk GNS LSB is displayed in **Figure 1C**. The absorption spectrum (**Figure 1D**, black spectrum) is dominated by the LSPR of the regular four branched component at 612 nm, with two shoulders at 530 nm (spheres) and at 760 nm (2- and 3-branched objects). The relatively short wavelength of the LSPR of the four branched regular nanostars is consistent with the base-to length ratio of their branches (0.9), very near to 1 and shifting of few tens of nm from the LSPR position of spherical Au nanoparticles, falling in the 520-550 nm range depending on their diameter (Kimling et al., 2006).

3.2. Coating of GNS with SH-PEG$_{3000}$-NH$_2$ and PPE-LA

Each of the three GNS types was coated with HS-PEG$_{3000}$-NH$_2$ (mw = 3000) and with PPE-LA. The latter is an amphiphilic copolymer prepared by our groups (Cavallaro et al., 2013), based on a biocompatible poly-(hydroxyethylaspartamide) (PHEA) backbone and bearing disulphide groups, PEG chains and amino groups, as illustrated in **Figure 2**.

Appending SH-PEG$_{3000}$-NH$_2$ and PPE-LA on GNS was obtained following our established procedures (Casu et al., 2012; Cavallaro et al., 2013; Pallavicini et al., 2015, 2013), using an excess of the coating polymers. This induces a small red shift (6-10 nm) of the LSPRs positions, due to the slight increase of the local refractive index brought by the grafted polymers (see **Figure S2(A-F)** in Supplementary material for spectra).

All the surfactants used in the synthesis and excess polymers are eliminated by three cycles of ultracentrifugation/redissolution (Borzenkov et al., 2015; Casu et al., 2012; Cavallaro et al., 2013; Pallavicini et al., 2013). After the last centrifugation, the pellet obtained from supernatant discarding is redissolved in a volume that is 1/10 of the starting one, to obtain concentrated solutions used for cellular treatments. The concentration of Au was determined for these final solutions as illustrated in the Experimental. Values are in the 0.17-0.33 mg Au/mL range; see **Table S2a** in Supplementary material for detailed values. It has to be noted that the complete redissolution of the pellet after many ultracentrifugation cycles is also a proof of the efficient and stable coating of GNS by the SH-PEG_{3000}-NH_2 and PPE-LA polymers. Control experiments were carried out on the three types of GNS with no addition of the coating polymers. In this case, as we have already observed (Casu et al., 2012; Pallavicini et al., 2013), ultracentrifugation caused aggregation of the GNS TRITON at the first cycle and of GNS LSB and shrunk GNS LSB at the second cycle, yielding a pellet that was not possible to redissolve in water even after 60 min of ultrasonication. In addition, ζ-potential measurements further confirmed the obtained coating. Beside the ζ-potential values measured in the condition of complexes formation (see section 3.3 and **Figure 3**), we also measured this parameter in strongly acidic (pH 3) and basic (pH 10) conditions, on GNS solutions of the three types, coated both with SH-PEG_{3000}-NH_2 and PPE-LA. The found ζ-potential values (see **Table S2b**) changed from very positive at pH 3 to slightly negative at pH 10, in correspondence of the amino groups protonation/deprotonation on the coating polymers. Such a behaviour wa already observed for GNS LSB coated with PPE-LA (Cavallaro et al., 2013) and SH-PEG_{3000}-NH_2 (Pallavicini et al., 2015).

Finally, although thermogravimetric and calorimetric measurements on coated GNS were not carried out, being outside the goals of this paper, from our previous data (Casu et al., 2012; Cavallaro et al., 2013; Pallavicini et al., 2013) we can roughly estimate the average number of coating polymers per GNS (see **S6** paragraph in Supplementary material section for

calculations). These are 24 and 60 PPE-LA units in the case of shrunk GNS LSB and GSN LSB, respectively, and 300, 750 and 10000 SH-PEG_{3000}-NH_2 units for shrunk GSN LSB, GSN LSB and GNS Triton, respectively. No data are available to calculate the number of PPE-LA units on GNS Triton.

3.3. Coated-GNS/siRNA complexes: preparation and characterization

GNS synthesized by using surfactants LSB and Triton-X 100 and coated with SH-PEG_{3000}-NH_2 or PPE-LA have a ζ-potential in bi-distilled water in the range 0 to + 40 mV (**Figure 3**). The starting ζ-potential for uncoated GNS is negative (~ -15 mV) (Casu et al., 2012; Cavallaro et al., 2013; Pallavicini et al., 2013) and these data demonstrated that gold nanoparticles were sufficiently coated with primary amine groups, which could be complexed with nucleic acids for efficient cellular uptake. The apparently surprising neutral ζ-potential of GNS LSB coated with PPE-LA (**Figure 3**) is due indeed to the slightly acidic pH at the end of the purification procedure (~ 6). We have already observed that ζ-potential of such PPE-LA coated GNS varies from +15 to – 15 mV as a function of pH and of amine protonation, with 0 mV corresponding to a condition in which ~ 50 % of the amino groups are protonated (Cavallaro et al., 2013). As nucleic acid model we chose a siRNA (siGL3) composed by 21bp, with a molecular weight of 13.3 kDa and a negative ζ potential in bidistilled water of ~ -20 mV. Upon interaction with siRNA molecules an inversion from positive to negative in the ζ potential of all coated GNS was observed (**Figure 4**), which indicates that an interaction occurred between the polymer coating and the siRNA. Starting from a certain siRNA/gold wt/wt ratio the zeta potential remained unchanged, likely due to a complete surface saturation by siRNA molecules. In particular, in the case of GNS LSB Shrunk+PEG-NH_2 and GNS LSB+PEG-NH_2 saturation occurred at lower weight ratios comprised between 0.066 and 0.1. At these weight ratios the ζ potential reached values up to -13 mV (**Figure 4A**). Surprisingly, GNS-TRITON+PEG-NH_2/siRNA seems to reach saturation above the highest weight ratio

tested, but after siRNA addition, samples displayed significant aggregation even with the addition of the smallest amount of siRNA tested, leading to the immediate sedimentation of the formed complexes (see **Figure S3** of Supplementary material). This is imputable to the surface charge close to neutrality that usually leads to aggregation due to the lack of electrostatic repulsion.

For PPE-LA coated GNS (GNS LSB+PPE-LA, GNS LSB Shrunk+PPE-LA and GNS TRITON+PPE-LA) saturation occurs at siRNA/gold wt/wt ratio between 0.2 and 1, for which the ζ potential reach values comprised between -17 and -20 mV (**Figure 4B**). The intensity-weighted diameters of all coated-GNS/siRNA complexes were also measured by DLS (**Figure 5**). After siRNA adsorption on all the three PPE-LA coated-GNS and on GNS LSB+PEG-NH_2, size was slightly affected. While the size of GNS LSB coated with either PPE-LA and SH-PEG_{3000}-NH_2 showed upon interaction with siRNA an increase of diameter of 11 and 13 nm on average respectively, in the case of GNS LSB Shrunk+PPE-LA and GNS TRITON+PPE-LA a little reduction of the diameter of about 4 nm was observed.

As consequence of aggregation, as discussed above, the largest increase in size following siRNA layering was observed with GNS TRITON+PEG-NH_2 with a diameter increase of 711 nm on average. GNS LSB Shrunk+PEG-NH_2 showed a gradual size increase with increasing siRNA/gold weight ratio used. In particular starting from 68.7 ± 37 nm of GNS LSB Shrunk+PEG-NH_2 size increase until 295 nm on average for wt ratios up to 0.066 wt ratio, and increase again up to 1100 on average in the ratio range between 0.1 and 1. In both cases, it is possible that siRNA addition promoted the formation of multi-GNS aggregates that further aggregated in larger structure starting from 0.066 wt ratio.

To effectively demonstrate siRNA interaction with GNS a comparative electrophoresis experiment has been carried out between two of the GNS tested in the work, i.e. GNS LSB+PEG-NH_2 and GNS TRITON+PEG-NH_2, and their negative counterpart, i.e. GNS LSB+PEG and GNS TRITON+PEG, in which a neutral SH-PEG (no –NH_2 terminal function)

has been used as coating. From this experiment is clear that while for positively charged systems a siRNA layering and retention occurred, in the case of SH-PEG coated GNS all the siRNA ran the gel as plain one (**Figure S5**).

3.4. Coated-GNS/siRNA complexes: In vitro biological characterization

Cytotoxicity is one of the most important factors to assess the siRNA carriers before they could be utilized for transfection study. The cell viability after treatment with the PPE-LA and SH-PEG_{3000}-NH_2 coated GNS/siRNA complexes at various siGL3 to gold weight ratios (ranging from 0.05 to 1) was compared with untreated control cells using MTS assay in MCF-7 cells after 24h incubation.

Results are reported in **Figure 6** and **7,** for PPE-LA and HS-PEG_{3000}-NH_2 coated GNS complexes respectively. In general it is possible to conclude that tested complexes are cytocompatible on this cell line, being the viability in the most of cases comprised between 80 and 100% respect to untreated cells. Nevertheless, there are some cases, corresponding to highest concentration of coated-GNS employed, in which is possible to note a slight decrease of cell viability down to 70%. At this regard it has to be pointed out the cytocompatibility experiments were carried out adding to the cell wells the same volume (200 μL) of coated-GNS/siGL3 complexes that had different siGL3/Au weight ratio, but always with an overall siGL3 concentration of 200 nM ($2.66 \cdot 10^{-3}$ mg/mL). In the case of the lowest weight ratio (0.05 siGL3/Au) this corresponds to a Au concentration as high as 0.053 mg/mL. At such concentrations, GNS LSB coated with SH-PEG_{3000}-NH_2 already demonstrated a similarly weak biotoxicity for SH-SY5Y neuroblastoma cells (Cavallaro et al., 2013).

The uptake of complexes and luciferase (Luc) gene silencing effect was evaluated at various siRNA to gold weight ratios on MCF-7/Luc cells, and normalized with respect to the overall cellular protein content. Left columns in **Figure 8** and **Figure 9** report the gene silencing efficiencies (RLU % down regulation) for GNS coated with PPE-LA and with SH-PEG_{3000}-

NH_2, respectively. Right columns of the same figures report instead the complexes uptake, measured on the basis of the fluorescence of the Cy5 fragment appended to siGL3. As shown in **Figure 8**, efficiency of silencing is similar after treatment with all PPE-LA coated GNS/siRNA.

The silencing effect is visible starting from weight ratio of 0.1 for GNS LSB+PPE-LA and GNS LSB SHRUNK+PPE-LA, and from weight ratio of 0.4 in the case of GNS TRITON+PPE-LA/siRNA, even if uptake starts to occur at lower weight ratio. The best result was achieved after treatment with GNS LSB+PPE-LA/siRNA at weight ratio of 0.4 (**Figure 8A**), with an extent of Luc expression of 56% when the Luc expression level of non-treated cells was set as 100%. With decreasing the weight ratio under 0.1 similar levels in the range 90-100% and over (no significant difference in a statistical t-test analysis with control) were observed.

Concerning siRNA efficiency after treatment with SH-PEG_{3000}-NH_2 coated GNS/siRNA complexes, down regulation assay results show how the greater efficiency of silencing is achieved after treatment with GNS LSB+PEG-NH_2 (left panel of **Figure 9A**). In particular, a significant reduction of luciferase expression up to 40%, is already visible at the lower siRNA to gold weight ratio (0.05) and the luciferase down regulation efficiency for GNS LSB+PEG-NH_2 increases with increasing weight ratio to achieve a reduction of luciferase activity up to about 25% for siGL3 to gold weight ratio of 1. Increasing the weight ratio increases the amount of siRNA interacting with coated GNS. Considering the previous zeta potential determination, this appears to arrive at full saturation starting from 0.1 weight ratio. Starting from this weight ratio, down regulation efficiency appears statistically almost unchanged, as can be seen in **Figure 9**, demonstrating in this case a correlation between siRNA/GNS interaction and gene silencing. Moreover, when down regulation efficiency for GNS LSB+PEG-NH_2 increased, the amount of siRNA taken up by cells was higher (right panel of **Figure 9A**).

In the case of GNS LSB SHRUNK+PEG-NH_2/siGL3 complexes (**Figure 9B**), the best result in terms of transfection efficiency was apparently obtained for the lower weight ratio, i.e. 0.05, with a reduction in recovered luminescence of about 80%. However, the data collected at 0.05 wt/wt are probably affected by a casual error, as they are not consistent with the smooth decreasing RLU trend observed with increasing wt/wt. Such a smooth trend is also in agreement with the smooth increase of the siGL3 cellular uptake observed in this case (right panel of **Figure 9B**).

It has to be stressed that the values of taken up siGL3 are in this case all in the 75000-110000 ng/mg protein, i.e. by far the highest when the SH-PEG_{3000}-NH_2 coating is used, in agreement with the better internalizing attitude of smaller (< 50 nm) nanoparticles (Jiang et al., 2008).

For GNS TRITON+PEG-NH_2 (**Figure 9C**) an effect on luciferase expression is visible for siRNA/gold weight ratio of 0.04 and 1. The siRNA down regulation effect, also in this case, appear to be higher when higher is the amount of GNS TRITON+PEG-NH_2/siRNA complexes taken up by cells (right panel of **Figure 9C**).

4. Discussion

AuNPs have the advantageous property of tuneable localized surface plasmon resonance (LSPR) (Pallavicini et al., 2011), an optical phenomenon that has been exploited for applications ranging from imaging and optical-based molecular detection to hyperthermal therapy for cancer treatment. Such a property is combined with facile synthetic methods and general biocompatibility (Tsai et al., 2015). Furthermore, thiol-Au chemistry provides an effective route for rational design by surface modification (i.e., attachment of functional macromolecules to the surface of AuNPs). As an exampl, by conjugation with functional copolymer ligands AuNPs can function as stealthy vectors to improve the delivery efficacy of many active substances such as conventional drugs or also Nucleic Acid Based Drugs (Muddineti et al., 2015). The concept of applying AuNPs in nanomedicine is attractive,

because in theory they can provide a therapeutic synergetic effect while avoiding or mitigating damage to healthy tissues. In order to achieve the desired functionality, it is necessary to identify and make use of AuNPs with suitable properties.

In the present study we have three GNS types with different encumbrance, belonging to three dimensional ranges: 80-90 nm (GNS TRITON), 50-70 nm (GNS LSB), 20-30 nm (shrunk GNS LSB), that we have coated with PPE-LA and SH-PEG_{3000}-NH_2. Both these cytocompatible polymers bear (1) anchoring groups (-SH or –S-S–) for grafting on the GNS surface, (2) amines (primary and/or secondary) to take advantage of their protonation at physiological pH and thus to ensure a positively charged surface for siRNA layering by electrostatic interactions, and (3) polyethylene glycol chains [-(OCH_2-CH_2)n-] because of their well-known ability to give colloidal stability and avoid recognition by the reticuloendothelial system. GNS LSB coated with SH-PEG_{3000}-NH_2 (Pallavicini et al., 2015) and with PPE-LA (Cavallaro et al., 2013) have been already reported by us. GNS TRITON and shrunk GNS LSB coated with PPE-LA and SH-PEG_{3000}-NH_2 are instead used for the first time in this paper. We demonstrated the applicability of polymer functionalized GNS for intracellular delivery of siRNA and highlighted the differences in GNS obtained by different synthetic procedures and coated with linear SH-PEG_{3000}-NH_2 with a terminal grafting point for Au or PEGylated PPE-LA graft copolymers offering a more complex structure and multiple grafting points (see **Figure 2**).

4.1. Colloidal stability

Colloidal stability is an important factor for the production and application of AuNPs. Agglomeration/aggregation is the principal result of poor colloidal stability, occurring due to different and often synergic factors and forces between AuNPs. This process directly leads to changes in the transport properties (circulation and transport across membranes) and also in the imaging/diagnostic and therapeutic performance of the material. In this comparative study

we measured size and surface charge modifications after siRNA interaction in the native water suspension, finding a correlation between colloidal stability, morphology (size and shape) and the nature of the ligand on the surface.

With PPE-LA, the PEG side chains on the polyaspartamide backbone ensure the colloidal stability of the formulation upon siRNA layering and prevent size alterations and aggregation phenomena. On the other hand, with the linear SH-PEG_{3000}-NH_2 colloidal stability of the complexes is not obtained in some of the examined cases. Uncontrollable aggregation on siRNA layering is observed in particular in the case of GNS TRITON+PEG-NH_2 and GNS LSB SHRUNK+PEG-NH_2. Factors affecting the colloidal stability of AuNPs include steric repulsion factors, electrostatic repulsion factors and their anisotropic nature (the tendency to aggregate is higher especially in case of large non-spherical particles such as GNS).

GNS TRITON+PEG-NH_2 aggregation during the siRNA layering process could be imputable to electrostatic factors since the surface potential upon siRNA addition falls to neutrality, thus justifying the formation of large aggregates. A contribution is expected also to come from the pronounced anisotropy due to branches length, which might favour the adhesion of large, flat surface portions. On the other hand, clustering effect during the siRNA layering process on GNS LSB SHRUNK+PEG-NH_2 could not be imputable to electrostatic repulsion factors only, since surface after siRNA interaction is negatively charged (ζ potential < -10 mV), but could be due also to multivalent interactions of siRNA, working as a bridge between multiple coated GNS. siRNA is a ≈ 13 KDa anionic biomolecule, capable of forming multi-cored aggregates whose size increases with increase in siRNA concentration. Also in this case anisotropy is expected to play a role, even if less than in the former case.

These differences in colloidal stability between SH-PEG_{3000}-NH_2 and PPE-LA coated GNS could ultimately be referred to the different nature of these two polymers. While PPE-LA is a graft amphiphilic copolymer able to form polymeric micelles by self-assembling in aqueous environment, PEG is a linear hydrophilic polymer. Linear PEG-conjugation via thiol-Au

bonding results in brush like coating (Tsai et al., 2015), while it is known from literature that amphiphilic copolymers could segregate AuNPs into the hydrophobic core during or after self-assembling in water and physically isolate them from its environment. For example, in a study performed by Taton and co-workers, AuNPs were encapsulated inside the polystyrene-b-poly(acrylic acid) (PS-b-PAA) micelles, which were further cross-linked in the polymer shells to obtain stable polymer/gold nanocomposites (Kang and Taton, 2005). In another study, micelles were obtained by using an amphiphilic copolymer with a long hydrophilic block which favoured single encapsulation of AuNPs (Chen et al., 2008). Moreover, we have already observed that with GNS LSB the % weight of the coating is higher in the case of PPE-LA (6.6%) (Cavallaro et al., 2013) than in the case of a HS-PEG with the same MW as that used here (4.4%) (Casu et al., 2012). This suggests that the coating layer on GNS+PPE-LA in water dispersion could form a thicker and complex layer and mitigate the difference between GNS LSB SHRUNK, GNS LSB and GNS TRITON in terms of anisotropy, size and surface charge upon siRNA interaction. This can be seen by comparing different PPE-LA coated GNS in graphs 4B and 5A where zeta potential and the size of complexes are reported. This similarity is not visible between the three SH-PEG_{3000}-NH_2 coated GNS in the corresponding graphs 4A and 5B.

4.2. Interaction with MCF-7 cells

More than just colloidal stability differences, PPE-LA coating suppresses also differences between different GNS types during transfection and gene silencing, leading to more homogeneous and consistent results. SH-PEG_{3000}-NH_2 coated GNS showed to have different behaviours by varying the synthetic method and then the type of GNS obtained. Mitigation of the dimensional differences due to PPE-LA coating with respect to SH-PEG_{3000}-NH_2 can be sharply seen in the GNS uptake: when coated with SH-PEG_{3000}-NH_2, the smaller GNS LSB SHRUNK nanostars enter more efficiently the MCF-7 cells with respect to GNS LSB and

GSN TRITON (**Figure 9**, right panels). When coated with PPE-LA such difference is not observed (**Figure 8**, right panel). Also these findings are interpreted by us as a consequence of the different rearrangement of copolymers on the GNS surface, and confirm the postulated formation of thicker and complex supramolecular layer and a segregation of differently structured GNS inside hydrophobic core able to mask such differences.

5. Conclusion

The siRNA complexes of all the coated gold nanoparticles tested were able to be internalized by MCF-7cells in a superior extent than siRNA alone. Furthermore, they efficiently suppressed Luciferase expression within the cells without eliciting severe cytotoxicity. This comparative study demonstrate the applicability of siRNA delivery by GNS, stating also that amphiphilic biocompatible polymers with multi-grafting function are more suitable for assuring the colloidal stability and effectiveness of these colloidal systems with respect to a typical PEG coating. This issue needs deeper insight considering that literature is scarce of information about GNS respect to investigation on spherical AuNPs. Considering the further potential therapeutic use of GNS (e.g. due to their NIR photothermal response), this could improve the effort that science does in the field of Au nanotechnology in biomedical applications, opening new perspectives to obtain clinically reliable systems.

Funding: This work was supported by the Italian Minister of Instruction, University and Research (MIUR) and PRIN 2010-11 [20109PLMH2]. The University of Pavia and CIRCMSB (Consorzio Interuniversitario di Ricerca in Chimica dei Metalli nei Sistemi Biologici) are also gratefully acknowledged for support.

6. References

Borzenkov, M., Chirico, G., D'Alfonso, L., Sironi, L., Collini, M., Cabrini, E., Dacarro, G., Milanese, C., Pallavicini, P., Taglietti, A., Bernhard, C., Denat, F., 2015. Thermal and Chemical Stability of Thiol Bonding on Gold Nanostars. Langmuir 31, 8081–91. doi:10.1021/acs.langmuir.5b01473

Casu, A., Cabrini, E., Donà, A., Falqui, A., Diaz-Fernandez, Y., Milanese, C., Taglietti, A., Pallavicini, P., 2012. Controlled synthesis of gold nanostars by using a zwitterionic surfactant. Chemistry 18, 9381–90. doi:10.1002/chem.201201024

Cavallaro, G., Triolo, D., Licciardi, M., Giammona, G., Chirico, G., Sironi, L., Dacarro, G., Donà, A., Milanese, C., Pallavicini, P., 2013. Amphiphilic copolymers based on poly[(hydroxyethyl)-D,L-aspartamide]: a suitable functional coating for biocompatible gold nanostars. Biomacromolecules 14, 4260–70. doi:10.1021/bm401130z

Chen, H.Y., Abraham, S., Mendenhall, J., Delamarre, S.C., Smith, K., Kim, I., Batt, C.A., 2008. Encapsulation of single small gold nanoparticles by diblock copolymers. Chemphyschem 9, 388–92. doi:10.1002/cphc.200700598

Freddi, S., Sironi, L., D'Antuono, R., Morone, D., Donà, A., Cabrini, E., D'Alfonso, L., Collini, M., Pallavicini, P., Baldi, G., Maggioni, D., Chirico, G., 2013. A Molecular Thermometer for Nanoparticles for Optical Hyperthermia. Nano Lett. 13, 2004–2010. doi:10.1021/nl400129v

Ghosh, P., Han, G., De, M., Kim, C.K., Rotello, V.M., 2008. Gold nanoparticles in delivery applications. Adv. Drug Deliv. Rev. 60, 1307–15. doi:10.1016/j.addr.2008.03.016

Greish, K., 2010. Enhanced permeability and retention (EPR) effect for anticancer nanomedicine drug targeting. Methods Mol. Biol. 624, 25–37. doi:10.1007/978-1-60761-609-2_3

Guerrero-Martínez, A., Barbosa, S., Pastoriza-Santos, I., Liz-Marzán, L.M., 2011. Nanostars shine bright for you: Colloidal synthesis, properties and applications of branched metallic nanoparticles. Curr. Opin. Colloid Interface Sci. 16, 118–127. doi:10.1016/j.cocis.2010.12.007

Huang, X., Jain, P.K., El-Sayed, I.H., El-Sayed, M.A., 2008. Plasmonic photothermal therapy (PPTT) using gold nanoparticles. Lasers Med. Sci. 23, 217–28. doi:10.1007/s10103-007-0470-x

Jiang, W., Kim, B.Y.S., Rutka, J.T., Chan, W.C.W., 2008. Nanoparticle-mediated cellular response is size-dependent. Nat. Nanotechnol. 3, 145–50. doi:10.1038/nnano.2008.30

Kang, Y., Taton, T.A., 2005. Core/Shell gold nanoparticles by self-assembly and crosslinking

of micellar, block-copolymer shells. Angew. Chem. Int. Ed. Engl. 44, 409–12. doi:10.1002/anie.200461119

Kimling, J., Maier, M., Okenve, B., Kotaidis, V., Ballot, H., Plech, A., 2006. Turkevich method for gold nanoparticle synthesis revisited. J. Phys. Chem. B 110, 15700–7. doi:10.1021/jp061667w

Lee, J., Chatterjee, D.K., Lee, M.H., Krishnan, S., 2014. Gold nanoparticles in breast cancer treatment: promise and potential pitfalls. Cancer Lett. 347, 46–53. doi:10.1016/j.canlet.2014.02.006

Lee, S.H., Bae, K.H., Kim, S.H., Lee, K.R., Park, T.G., 2008. Amine-functionalized gold nanoparticles as non-cytotoxic and efficient intracellular siRNA delivery carriers. Int. J. Pharm. 364, 94–101. doi:10.1016/j.ijpharm.2008.07.027

Liu, Y., Yuan, H., Kersey, F.R., Register, J.K., Parrott, M.C., Vo-Dinh, T., 2015. Plasmonic gold nanostars for multi-modality sensing and diagnostics. Sensors (Basel). 15, 3706–20. doi:10.3390/s150203706

Massich, M.D., Giljohann, D.A., Seferos, D.S., Ludlow, L.E., Horvath, C.M., Mirkin, C.A., 2009. Regulating immune response using polyvalent nucleic acid-gold nanoparticle conjugates. Mol. Pharm. 6, 1934–40. doi:10.1021/mp900172m

Muddineti, O.S., Ghosh, B., Biswas, S., 2015. Current trends in using polymer coated gold nanoparticles for cancer therapy. Int. J. Pharm. 484, 252–67. doi:10.1016/j.ijpharm.2015.02.038

Nikoobakht, B., El-Sayed, M.A., 2003. Preparation and Growth Mechanism of Gold Nanorods (NRs) Using Seed-Mediated Growth Method. Chem. Mater. 15, 1957–1962. doi:10.1021/cm0207321

Pallavicini, P., Cabrini, E., Cavallaro, G., Chirico, G., Collini, M., D'Alfonso, L., Dacarro, G., Donà, A., Marchesi, N., Milanese, C., Pascale, A., Sironi, L., Taglietti, A., 2015. Gold nanostars coated with neutral and charged polyethylene glycols: A comparative study of in-vitro biocompatibility and of their interaction with SH-SY5Y neuroblastoma cells. J. Inorg. Biochem. 151, 123–31. doi:10.1016/j.jinorgbio.2015.05.002

Pallavicini, P., Chirico, G., Collini, M., Dacarro, G., Donà, A., D'Alfonso, L., Falqui, A., Diaz-Fernandez, Y., Freddi, S., Garofalo, B., Genovese, A., Sironi, L., Taglietti, A., 2011. Synthesis of branched Au nanoparticles with tunable near-infrared LSPR using a zwitterionic surfactant. Chem. Commun. (Camb). 47, 1315–7. doi:10.1039/c0cc02682d

Pallavicini, P., Donà, A., Casu, A., Chirico, G., Collini, M., Dacarro, G., Falqui, A., Milanese, C., Sironi, L., Taglietti, A., 2013. Triton X-100 for three-plasmon gold nanostars with

two photothermally active NIR (near IR) and SWIR (short-wavelength IR) channels. Chem. Commun. (Camb). 49, 6265–7. doi:10.1039/c3cc42999g

Perche, F., Yi, Y., Hespel, L., Mi, P., Dirisala, A., Cabral, H., Miyata, K., Kataoka, K., 2016. Hydroxychloroquine-conjugated gold nanoparticles for improved siRNA activity. Biomaterials 90, 62–71. doi:10.1016/j.biomaterials.2016.02.027

Rahme, K., Guo, J., Holmes, J.D., O'Driscoll, C.M., 2015. Evaluation of the physicochemical properties and the biocompatibility of polyethylene glycol-conjugated gold nanoparticles: A formulation strategy for siRNA delivery. Colloids Surf. B. Biointerfaces 135, 604–12. doi:10.1016/j.colsurfb.2015.08.032

Tsai, D.-H., Lu, Y.-F., DelRio, F.W., Cho, T.J., Guha, S., Zachariah, M.R., Zhang, F., Allen, A., Hackley, V.A., 2015. Orthogonal analysis of functional gold nanoparticles for biomedical applications. Anal. Bioanal. Chem. 407, 8411–22. doi:10.1007/s00216-015-9011-9

Wang, B.-K., Yu, X.-F., Wang, J.-H., Li, Z.-B., Li, P.-H., Wang, H., Song, L., Chu, P.K., Li, C., 2016. Gold-nanorods-siRNA nanoplex for improved photothermal therapy by gene silencing. Biomaterials 78, 27–39. doi:10.1016/j.biomaterials.2015.11.025

Yuan, H., Fales, A.M., Vo-Dinh, T., 2012. TAT Peptide-Functionalized Gold Nanostars: Enhanced Intracellular Delivery and Efficient NIR Photothermal Therapy Using Ultralow Irradiance. J. Am. Chem. Soc. 134, 11358–11361. doi:10.1021/ja304180y

Zhao, X., Huang, Q., Jin, Y., 2015. Gold nanorod delivery of LSD1 siRNA induces human mesenchymal stem cell differentiation. Mater. Sci. Eng. C. Mater. Biol. Appl. 54, 142–9. doi:10.1016/j.msec.2015.05.013

FIGURE CAPTIONS

Figure 1. Transmission Electron Microscopy (TEM). A: TEM image of GNS LSB. B: TEM image of GNS TRITON. C: TEM image of shrunk GNS LSB. D: extinction spectra of the colloidal solutions of uncoated GNS LSB (red), GNS TRITON (blue), and shrunk GNS LSB (black).

Figure 2. Formula of the two GNS polymer coatings, PPELA and HS-PEG-NH_2.

Figure 3. ζ Potential of Gold Nanostars synthesized by using surfactants LSB and Triton-X 100 and coated with HS-PEG_{3000}-NH2 or PPE-LA, measured by DLS.

Figure 4. ζ Potential trend after addition of increasing amount of siRNA to Gold nanostars synthesized by using surfactants LSB and Triton-X 100 and coated with A) HS-PEG_{3000}-NH_2 or B) PPE-LA, measured by DLS.

Figure 5. Size variation of Gold nanostars synthesized by using surfactants LSB and Triton-X 100 and coated with **A**) PPE-LA or **B**) HS-PEG_{3000}-NH_2, after addition of increasing amount of siRNA, measured by DLS.

Figure 6. Cytocompatibility of PPE-LA coated GNS complexes, after 24h incubation on MCF-7 cells. A) GNS LSB SHRUNK+PPE-LA; B) GNS LSB+PPE-LA; C) GNS TRITON+PPE-LA. The data are reported as means ± standard deviation.

Figure 7. Citocompatibility of HS-PEG_{3000}-NH_2 coated GNS complexes, after 24h incubation on MCF-7 cells. A) GNS LSB SHRUNK+PEG-NH_2; B) GNS LSB+PEG-NH_2; C) GNS TRITON+PEG-NH_2. The data are reported as means ± standard deviation.

Figure 8. Luciferase down regulation efficiencies and uptake of siGL3-Cy5 carried by PPE-LA coated GNS complexes, after 24h incubation. A) GNS LSB+PPE-LA; B) GNS LSB SHRUNK+PPE-LA; C) GNS TRITON+PPE-LA. The data are reported as means ± standard deviation (symbol * indicates a significant difference respect to control (NT) ($p< 0.05$).

Figure 9. Luciferase down regulation efficiencies and uptake of siGL3-Cy5 carried by HS-PEG3000-NH_2 coated GNS complexes, after 24h incubation. A) GNS LSB+PEG-NH2; B) GNS LSB SHRUNK+PEG-NH_2; C) GNS TRITON+PEG-NH_2. The data are reported as means ± standard deviation (symbol * indicates a significant difference respect to control (NT) ($p< 0.05$).

FIGURES

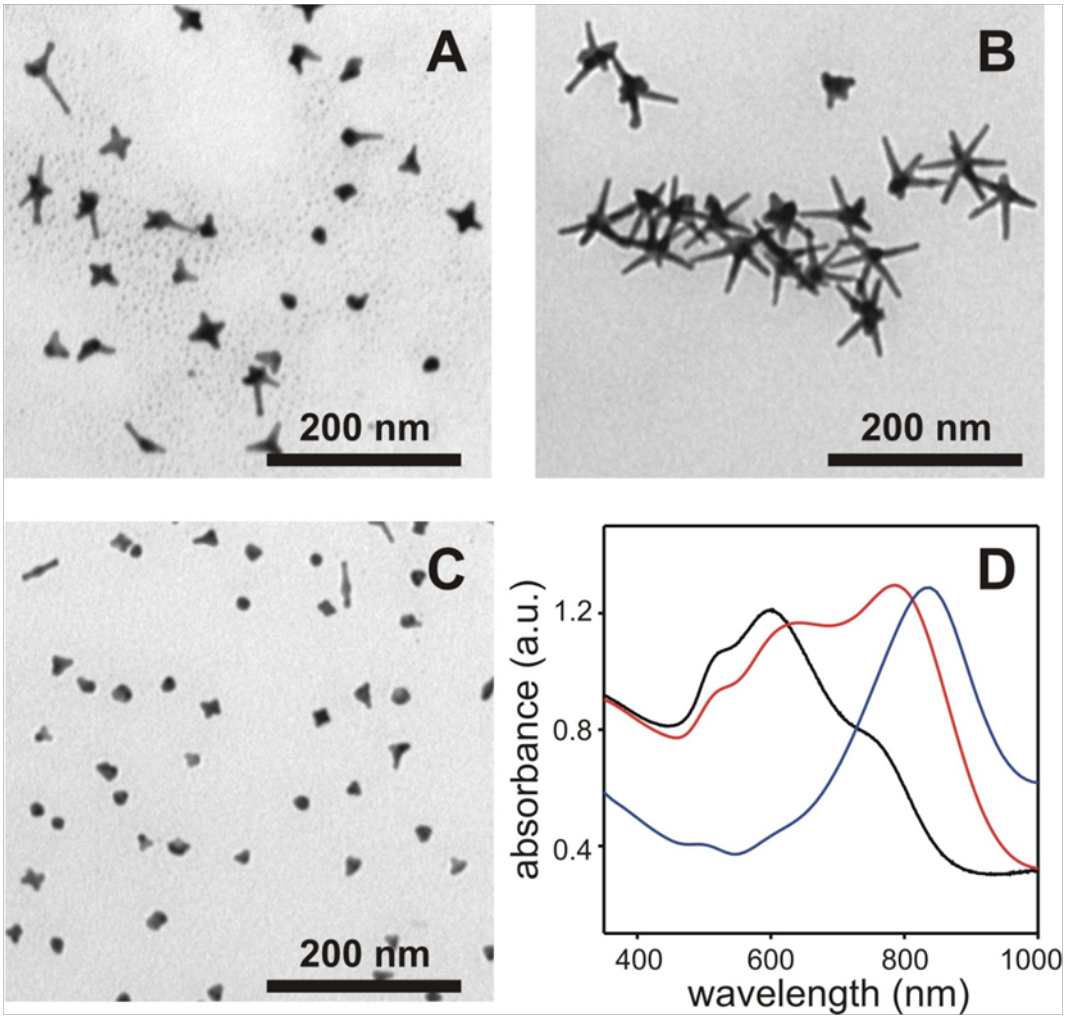

Figure 1

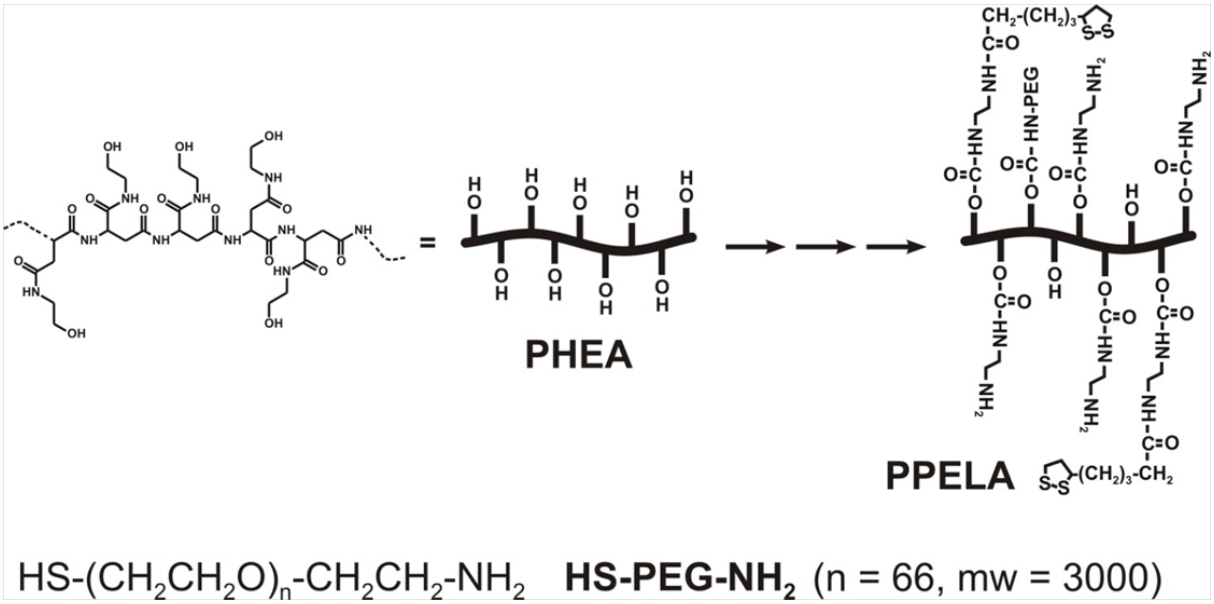

Figure 2

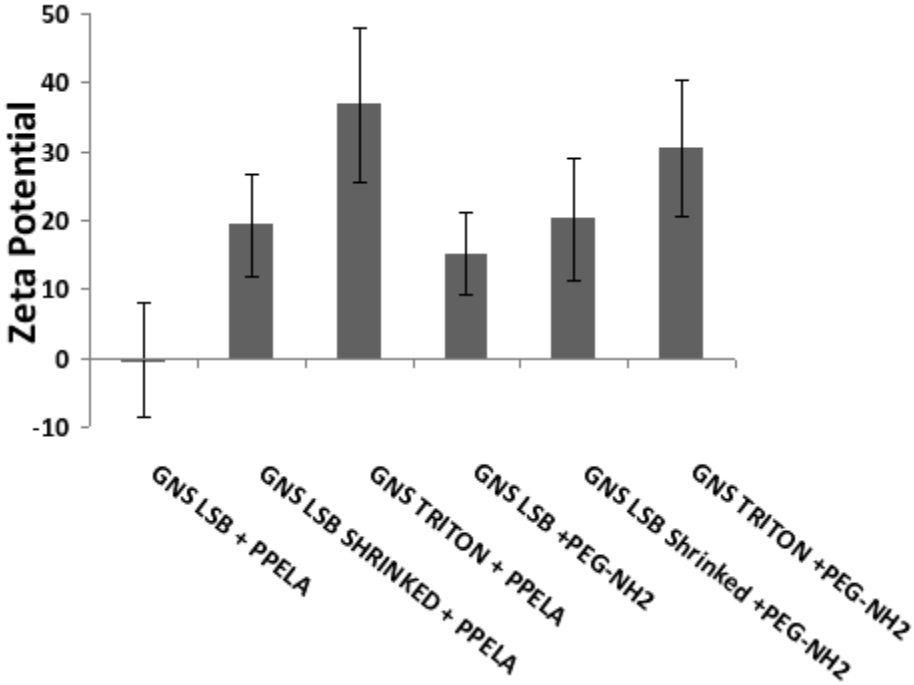
Zeta Potential
50
40
30
20
10
0
-10
GNS LSB + PPELA
GNS LSB SHRINKED + PPELA
GNS TRITON + PPELA
GNS LSB +PEG-NH2
GNS LSB Shrinked +PEG-NH2
GNS TRITON +PEG-NH2

Figure 3

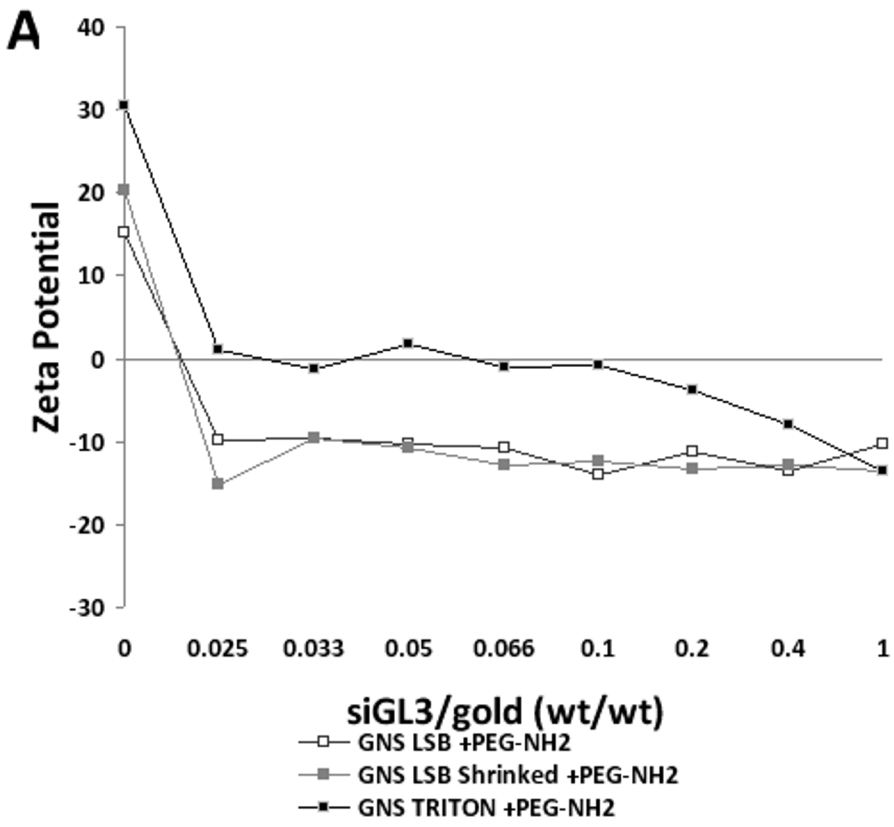
A
Zeta Potential
40
30
20
10
0
-10
-20
-30
0
0.025
0.033
0.05
0.066
0.1
0.2
0.4
1
siGL3/gold (wt/wt)
GNS LSB +PEG-NH2
GNS LSB Shrinked +PEG-NH2
GNS TRITON +PEG-NH2

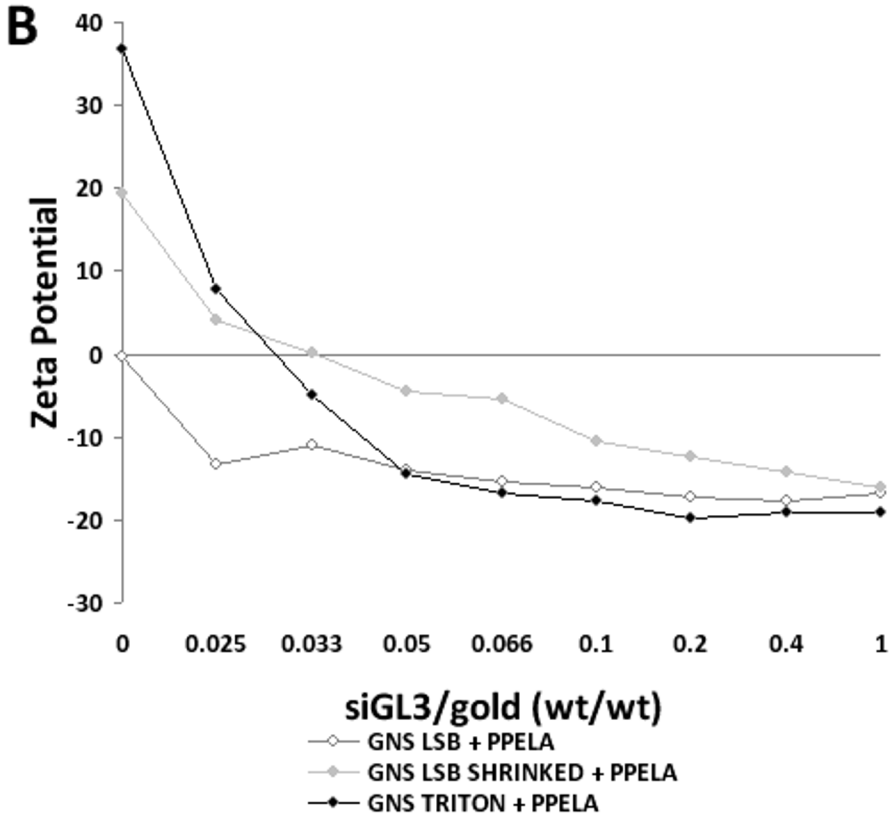
B
Zeta Potential
40
30
20
10
0
-10
-20
-30
0
0.025
0.033
0.05
0.066
0.1
0.2
0.4
1
siGL3/gold (wt/wt)
GNS LSB + PPELA
GNS LSB SHRINKED + PPELA
GNS TRITON + PPELA

Figure 4

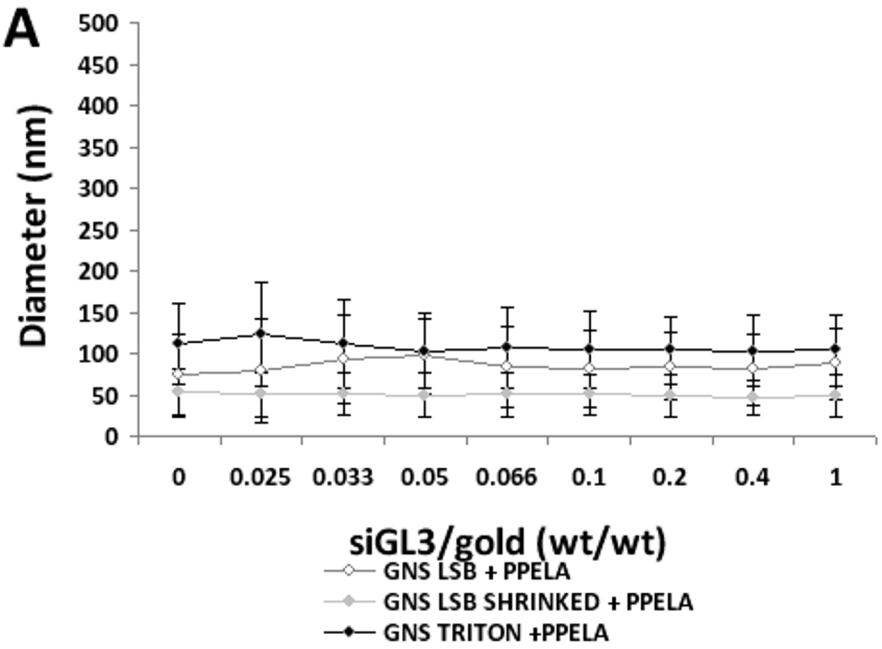
A
Diameter (nm)
500
450
400
350
300
250
200
150
100
50
0
0
0.025
0.033
0.05
0.066
0.1
0.2
0.4
1
siGL3/gold (wt/wt)
GNS LSB + PPELA
GNS LSB SHRINKED + PPELA
GNS TRITON +PPELA

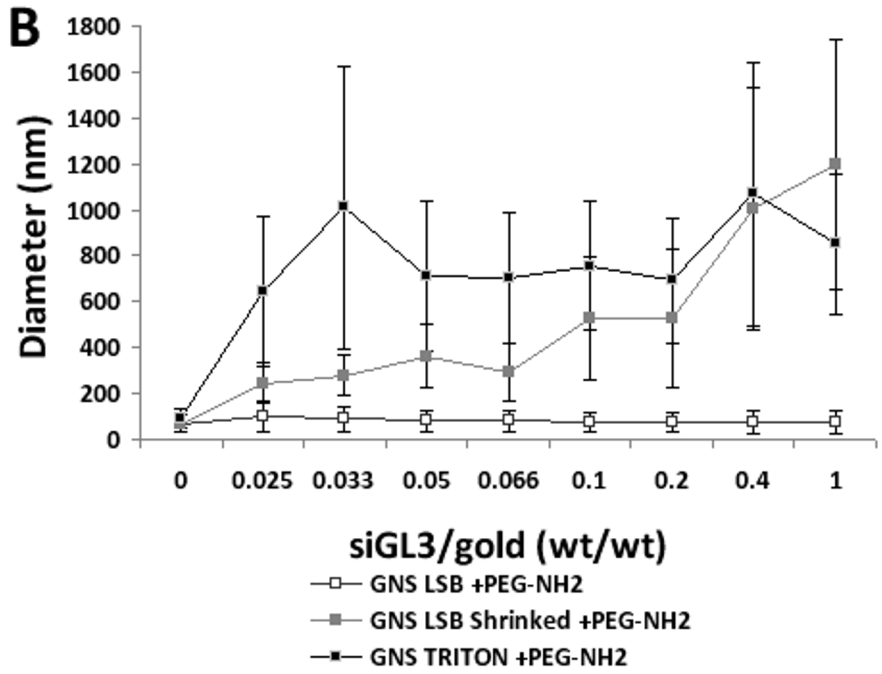
B
Diameter (nm)
1800
1600
1400
1200
1000
800
600
400
200
0
0
0.025
0.033
0.05
0.066
0.1
0.2
0.4
1
siGL3/gold (wt/wt)
GNS LSB +PEG-NH2
GNS LSB Shrinked +PEG-NH2
GNS TRITON +PEG-NH2

Figure 5

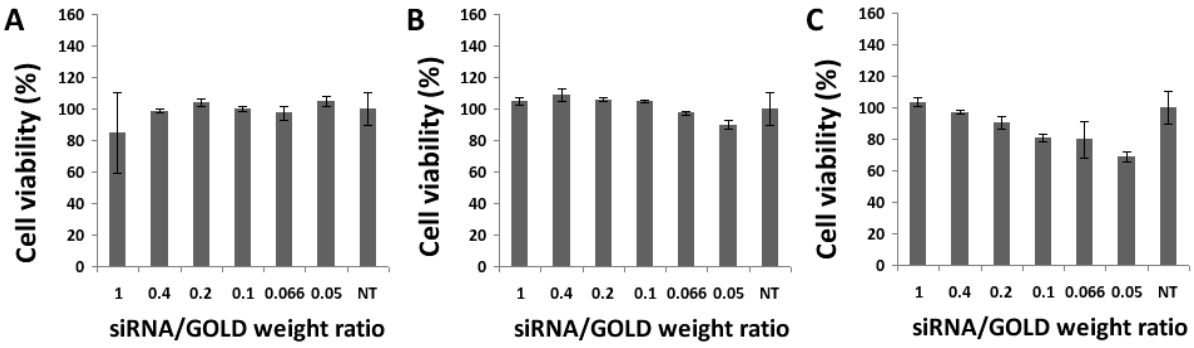
A
B
C
Cell viability (%)
160
140
120
100
80
60
40
20
0
1
0.4
0.2
0.1
0.066
0.05
NT
siRNA/GOLD weight ratio

Figure 6

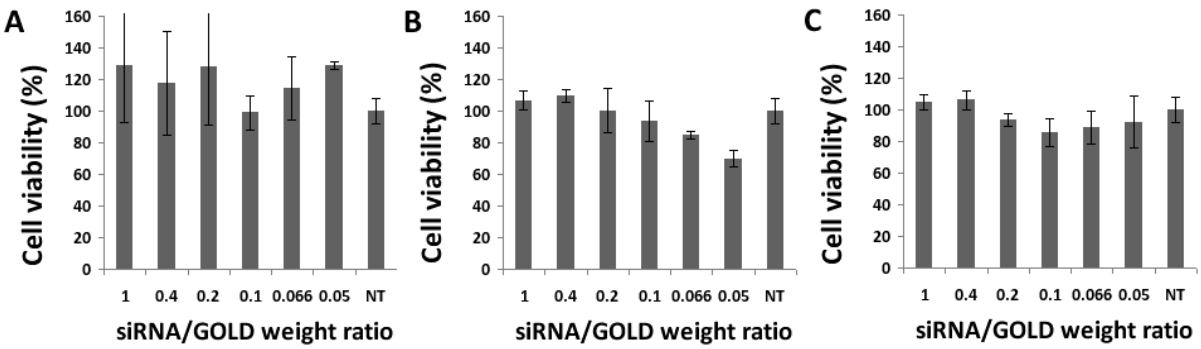
A
B
C
Cell viability (%)
160
140
120
100
80
60
40
20
0
1
0.4
0.2
0.1
0.066
0.05
NT
siRNA/GOLD weight ratio

Figure 7

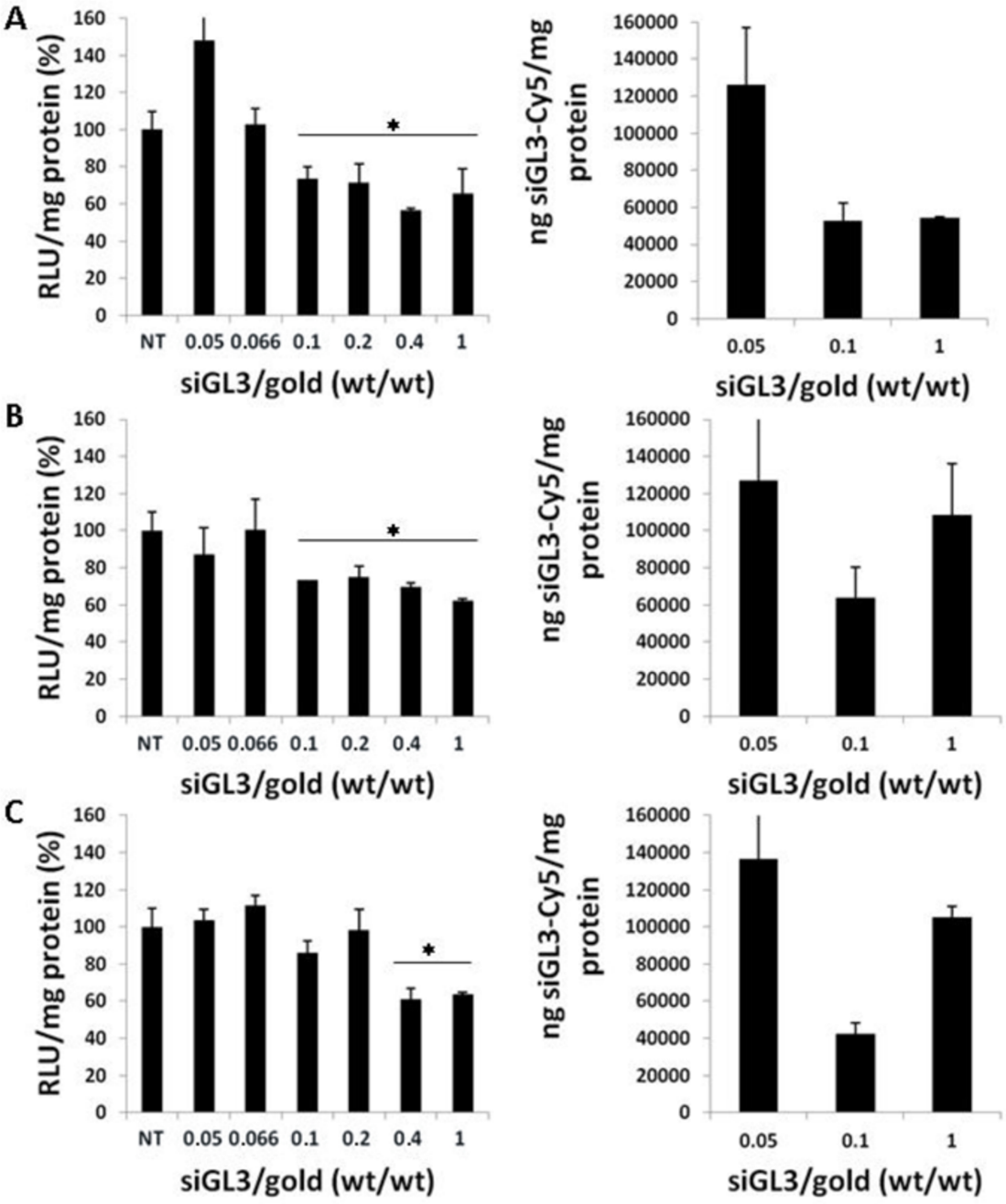
A
RLU/mg protein (%)
160
140
120
100
80
60
40
20
0
NT 0.05 0.066 0.1 0.2 0.4 1
siGL3/gold (wt/wt)
*
ng siGL3-Cy5/mg protein
160000
140000
120000
100000
80000
60000
40000
20000
0
0.05 0.1 1
siGL3/gold (wt/wt)
B
RLU/mg protein (%)
NT 0.05 0.066 0.1 0.2 0.4 1
siGL3/gold (wt/wt)
*
ng siGL3-Cy5/mg protein
0.05 0.1 1
siGL3/gold (wt/wt)
C
RLU/mg protein (%)
NT 0.05 0.066 0.1 0.2 0.4 1
siGL3/gold (wt/wt)
*
ng siGL3-Cy5/mg protein
0.05 0.1 1
siGL3/gold (wt/wt)

Figure 8

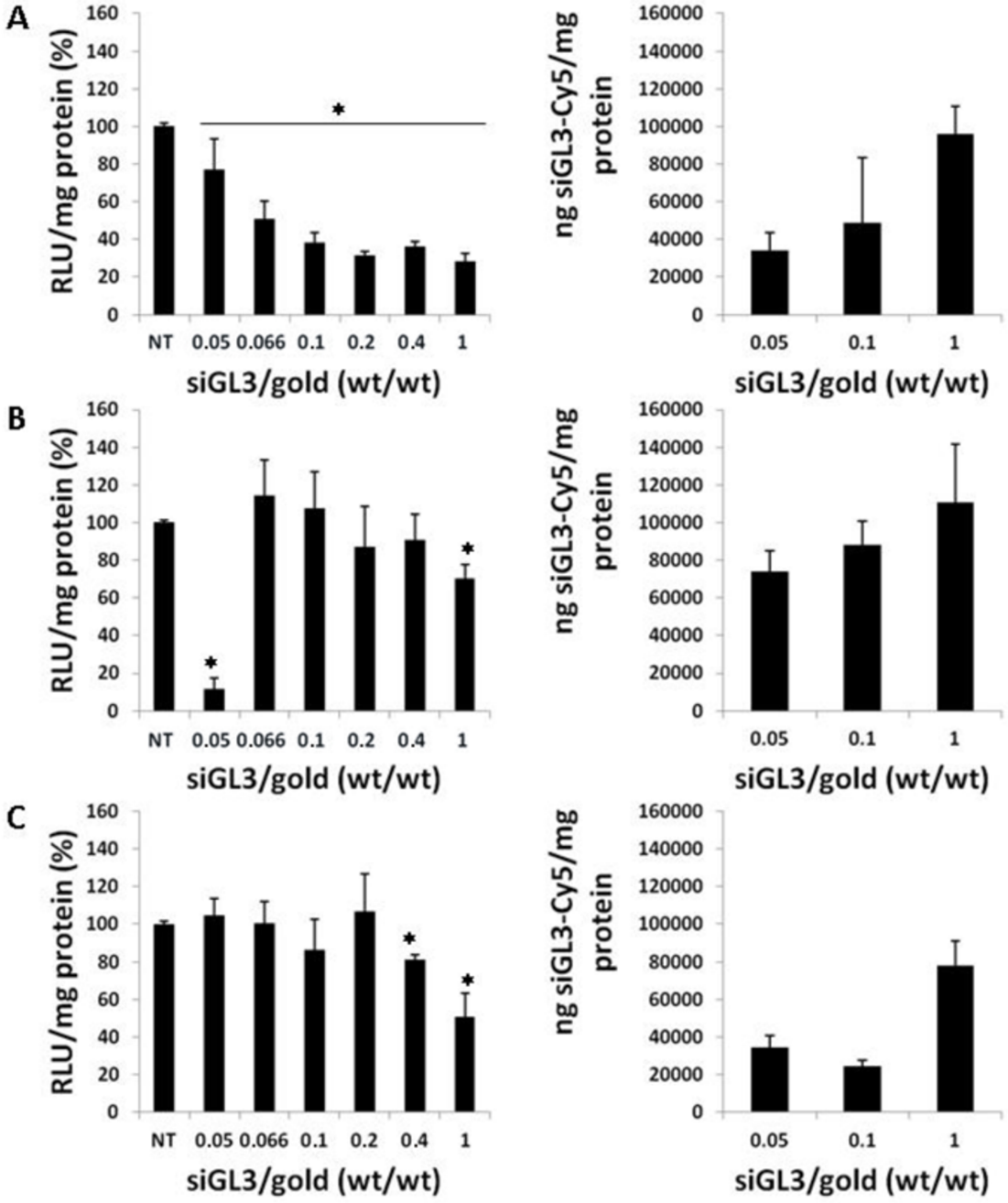
A
RLU/mg protein (%)
160
140
120
100
80
60
40
20
0
NT 0.05 0.066 0.1 0.2 0.4 1
siGL3/gold (wt/wt)
ng siGL3-Cy5/mg protein
160000
140000
120000
100000
80000
60000
40000
20000
0
0.05 0.1 1
siGL3/gold (wt/wt)
B
RLU/mg protein (%)
NT 0.05 0.066 0.1 0.2 0.4 1
siGL3/gold (wt/wt)
ng siGL3-Cy5/mg protein
0.05 0.1 1
siGL3/gold (wt/wt)
C
RLU/mg protein (%)
NT 0.05 0.066 0.1 0.2 0.4 1
siGL3/gold (wt/wt)
ng siGL3-Cy5/mg protein
0.05 0.1 1
siGL3/gold (wt/wt)

Figure 9